

CRYSTALLOGRAPHIC PROPERTIES OF $Sr_2NaNb_5O_{15}$ SYNTHESIZED BY MODIFIED POLYOL METHOD

S. A. Dantas *, S. Lanfredi, L. O. Salmazo, A. R. F. Lima, M. A. L. Nobre
Faculdade de Ciências e Tecnologia – FCT
Universidade Estadual Paulista
Departamento de Física, Química e Biologia – DFQB
Laboratório de Compositos e Cerâmicas Funcionais – LaCCeF
R. Roberto Simonsen 305, C. P. 467, Presidente Prudente, SP 19060-900
*samara_dadantas@yahoo.com

ABSTRACT

Ceramic materials with tetragonal tungsten bronze-TTB type structure are of great scientific and technical-industrial interest as materials for application in pyroelectric detectors and piezoelectric transducers. In this work were investigated the preparation and structural characterization of the sodium strontium niobate with $Sr_2NaNb_5O_{15}$ stoichiometry prepared by modified polyol method. The parameters time and calcination temperature to obtain $Sr_2NaNb_5O_{15}$ nanopowders were monitored by X-ray diffraction. Structural parameters and chemical bonds were investigated using the Rietveld method and FTIR spectroscopy, respectively. The average crystallite size of the precursor powder of $Sr_2NaNb_5O_{15}$, as a function of the thermal treatment time showed values between 36 and 42 nm. The crystallographic properties of the $Sr_2NaNb_5O_{15}$ are discussed.

Key-words: niobate, modified polyol method, Rietveld method, average crystallite size, FTIR spectroscopy.

INTRODUCTION

From ferroelectricity discovery and related properties in BaTiO₃, a large amount of research has been addressed to new ferroelectric oxides and properties, in the search by materials for technological applications ⁽¹⁾. High performance dielectric ceramics act as a key materials for resonators, temperature compensated capacitors and thermistors. Another set ferroelectric polycation oxides are also interesting due to the microwave telecommunications progress involving satellite broadcasting and other related devices ⁽²⁾. Technological research on the next generation of wireless telecommunications devices has revealed a lack of proper materials for use in new electronic elements and devices. This lack of advanced materials represents a challenge to development of next generation of materials to the microwave application. An among ferroelectric oxides, especially some lead-free oxides with the tetragonal tungsten bronze structure (TTB) type are in forefront both in the area of research as well as in industrial applications. Taking into account structure TTB type, a wide variety of cations substitution is possible due the presence of several interstices called A, B, and C, respectively ^(3,4). The tetragonal tungsten bronze (TTB) structure type can be considered as a derivative of the classical perovskite one. It can be described by the chemical formula (A1)₂(A2)₄C₄Nb₁₀O₃₀, where A1, A2, and C denote different sites in the crystalline structure. The A1 cavities have a cuboctahedral coordination of oxygen atoms, the A2 cavities a pentacapped pentagonal prismatic, and the C cavities a tricapped trigonal prismatic one. The size of these cavities decreases in the order A2 > A1 > C. TTB type compounds, alkaline and/or alkaline-earth metals are located in the A1 and A2 sites, while only small cations like Li are found in the C site ⁽⁵⁾. TTB-type compounds with A₆Nb₁₀O₃₀ formulae, with A = Sr, Ba, are semiconductors containing niobium ions. In part the semiconducting behavior of these compounds might be due the low electron concentration compared to the Na_{4.5}W₁₀O₃₀ metallic. However, the increase of the number of charge carries is possible by the replacing specific divalent alkaline earth cations by trivalent lanthanoids one, in according to rule gives by the M²⁺_{6-x}Ln³⁺_xNb₁₀O₃₀ formula. Particular distribution of metal cations in different interstices can improve physical properties, such as electro-optic, nonlinear, elasto-optic and pyroelectric properties ⁽⁶⁾. These properties depend on the powder morphology and the method of synthesis.

EXPERIMENTAL PROCEDURE

Nanostructured $\text{Sr}_2\text{NaNb}_5\text{O}_{15}$ single phase powder was synthesized by the Modified Polyol method. As a whole, this method gives rise a better control of reagents, a low calcination temperature, a single phase material and powder with high specific surface area. The starting reagents for the powder synthesis via chemical route were nitric acid HNO_3 (99.5% Reagen), strontium carbonate SrCO_3 (99.0% Reagen), sodium carbonate Na_2CO_3 (99.0% Reagen), ethylene glycol $\text{HOCH}_2\text{CH}_2\text{OH}$ (98.0% Synth) and niobium ammonium oxalate $\text{NH}_4\text{H}_2[\text{NbO}(\text{C}_2\text{O}_4)_3] \cdot 3\text{H}_2\text{O}$ (CBMM-Brazil). All salts were dissolved in nitric acid with continuous stir in a beaker. In the sequence, 100 ml of ethylene glycol was added. The solution was heated at 90 °C, promoting the decomposition of NO_3 group, similar to the process developed in the Pechini method ⁽⁷⁾. After the polyesterification reaction, a polymeric gel is obtained. The polymer is maintained in the beaker undergoes a primary calcinations in a furnace type box. The heating cycle was carried out via two calcinations steps, in N_2 atmosphere with flux of 500 ml/min. From room temperature, the temperature was increased using a heating rate equal to 10 °C/min up to 150 °C at this point the temperature was kept constant during 30 min. In the sequence, the same heating rate was used to increase the temperature at 300 °C, being maintained during 1 hour. After this cycle, the furnace was cooling to the natural rate. The nitrogen flux was constant at 500 ml/min during the cooling cycle. This process leads to the partial polymer decomposition forming a resin, which consist in a brittle reticulated material. This material was deagglomerate in an agate mortar being termed precursor. The precursor was calcinated in a tube furnace in oxygen atmosphere. The time and temperature parameters, of the precursor powder, were optimized to obtain $\text{Sr}_2\text{NaNb}_5\text{O}_{15}$ single phase powders with high crystallinity. The calcinations was carried out in the temperatures range from 350 to 1150 °C during 4, 6, 8, 10 and 12 hours, using heating rate equal to 5 °C/min, with oxygen flux of 300 mL/min.

The starting reagents for preparation of the precursor powder were: hydrated niobium oxide ($\text{Nb}_2\text{O}_5 \cdot 4\text{H}_2\text{O}$), sodium carbonate (Na_2CO_3), strontium carbonate (SrCO_3) and isopropyl alcohol, all P.A. reagents.

The characteristics of the starting reagents are shown in Table 1.

Table 1. Characteristics of the starting reagents.

Name	Formula	Molecular weight	Origin
Hydrated niobium oxide	$\text{Nb}_2\text{O}_5 \cdot 4\text{H}_2\text{O}$	345.62	CBMM - Araxá
Sodium carbonate	Na_2CO_3	105.99	VETEC
Strontium carbonate	SrCO_3	147.63	VETEC
Isopropyl alcohol	$(\text{CH}_3)_2\text{CHOH}$	60.10	VETEC

Structural Characterization

Chemical bonds were analyzed by FTIR spectroscopy. The samples were diluted in KBr in a ratio of 1:100. Measurements were carried out in the range of $1000\text{--}400\text{ cm}^{-1}$ with 100 scans, using a Fourier Transform spectrometer Model Digilab Excalibur (FTS 3100 HE series). The peak positions were determined using the PeakFit. Program.

Structural characterization of the $\text{Sr}_2\text{NaNb}_5\text{O}_{15}$ powder was carried out by X-ray diffraction (XRD). A Shimadzu (model D-6000) diffractometer with $\text{Cu-K}\alpha$ radiation ($\lambda = 1.54\text{ \AA}$) was used. Measurements were carried out in the angular range $5^\circ \leq 2\theta \leq 80^\circ$ with a scanning step of 0.02° . The diffraction pattern was refined according to the Rietveld method using the Fullprof program⁽⁸⁾. Parameters and variables adopted during the refinement process were the background coefficients, profile coefficients, histogram scale, lattice parameters, linear absorption coefficients, coordination parameters or oxygen parameters (X), and isothermal parameters for four kinds of atoms (Na, Sr, Nb, and O). The background level was fitted with a five-order polynomial function, and the peak shape, with a pseudo-Voigt function. The angular dependence of the peak full-width at half-maximum (H) was defined by the function determined by Caglioti⁽⁹⁾. From atomic positions derived in the refinement step, the $\text{Sr}_2\text{NaNb}_5\text{O}_{15}$ unit cell was built using the Diamond software package⁽¹⁰⁾. The average crystallite size (D) and the lattice strain of $\text{Sr}_2\text{NaNb}_5\text{O}_{15}$ were estimated from X-ray diffraction line broadening. The crystallite size was estimated by Scherrer's equation using the Jade 8 Plus software⁽¹¹⁾:

$$D = \frac{k \cdot \lambda}{\beta \cdot \cos \theta} \quad (\text{A})$$

where β is the broadening of the diffraction line measured at half-maximum intensity, λ is the wavelength (Cu-K α), θ is the Bragg angle for a given diffraction, and k is a constant, in general equal to 0.9 for powders. The calculated crystallite size was equal to 36 nm. The instrumental broadening effect was eliminated by subtracting the value of full width at half-maximum (β_0) corresponding to a standard sample (SiO₂) from β of the respective Bragg peaks.

RESULTS AND DISCUSSION

Bond Analysis

Figure 1 shows the FT-IR spectrum of the Sr₂NaNb₅O₁₅ powder. It presents eight bands positioned at 414, 472, 538, 604, 667, 728, 783, and 844 cm⁻¹, all bands assigned to Nb–O bond. Six of them which are broad, asymmetric, and of middle intensity are centered at 538, 604, 667, 728, 783, and 844 cm⁻¹, respectively. The other two bands are sharp with low intensity, centered at 472, and 414 cm⁻¹, respectively.

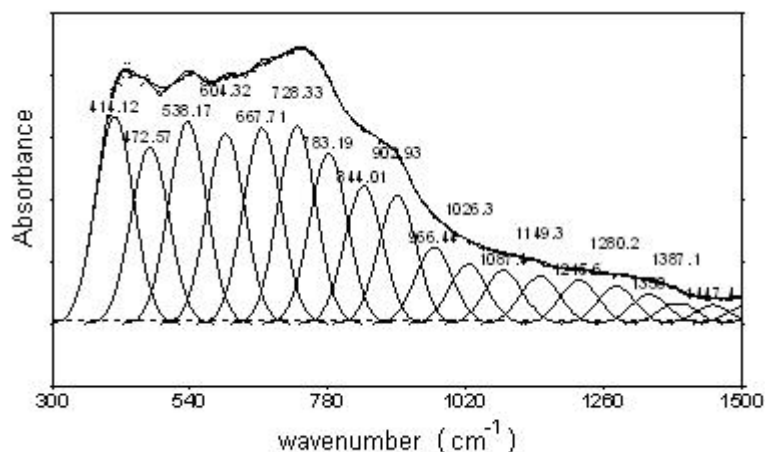


Figure 1. FT-IR spectra of the Sr₂NaNb₅O₁₅ powder.

The absorption band assignment is shown in Table 2. The vibration involving Nb terminal O bond should give an absorption band at higher frequency (small wavenumber $1/\lambda$ or less energetic side of spectrum) than a Nb–O–Nb bond, and *vice-versa*. Sharp absorption bands of low intensity at 472 cm^{-1} and 414 cm^{-1} have also been assigned to Nb–O stretching ⁽¹²⁾, of the niobium bond with apical oxygen in the $[\text{NbO}_6]$ octahedron. The band positioned between 783 cm^{-1} and 538 cm^{-1} were assigned to symmetric Nb–O–Nb stretching. The absorption band centered at 844 cm^{-1} was assigned to the Nb–O stretching ⁽¹³⁾. The band assigned to Nb–O stretching ⁽¹²⁾ is particularly important, since has been assigned to niobium bond with apical oxygen in the $[\text{NbO}_6]$ octahedron.

Table 2. Assignment of FT-IR absorption bands.

Assignments	Wavenumber (cm^{-1})	Intensity	Ref.
Stretching of the Nb–O bonds *	472, 414	low	12, 13
Nb–O–Nb vibrational mode *	783 - 538	medium	12
Stretching of the Nb–O bonds **	844	low	

* NbO_6 Octahedra

**Distorted NbO_6 Octahedra, Nb bond with apical oxygen

Phase Formation

The $\text{Sr}_2\text{NaNb}_5\text{O}_{15}$ nanostructured powder exhibited only a set of diffraction lines, which was ascribed to the TTB-type structure identified from the JCPDS card number 34-0429. As expected, the major crystallinity was attained with thermal treatment at $1150\text{ }^\circ\text{C}$ for 12 h. The average crystallite size (D) was derived as a function of the calcination time. The corresponding values are showed in Figure 2. D parameter was derived in accordance with Eq. (A). As shown in Figure 2, the evolution of the average crystallite size occurred in some steps. A small increase of the crystallite size was accomplished as a function of temperature. The lowest average crystallite size was observed after 6 h of thermal treatment, $D = 35\text{ nm}$.

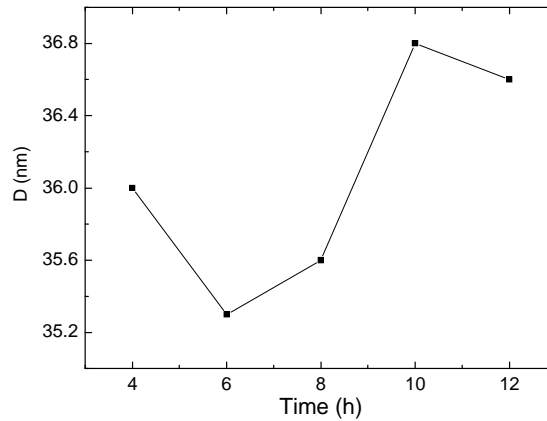


Figure 2. Average crystallite size as a function of the time.

Counterclockwise, the highest average crystallite size, at around 36.7 nm, was derived for the $\text{Sr}_2\text{NaNb}_5\text{O}_{15}$ precursor powder calcined for 12 h. In this way, the increase of the average crystallite size as a function of the thermal treatment time correlated with the thermal activation of the mass transport mechanism at 1150 °C, which may be related to a systematic increase of the defect elimination kinetics in the material, as well as a small variation of the degree of microstrain.

Rietveld Refinement

The X-ray diffraction pattern was indexed on the basis of a tetragonal unit cell. The structural parameter set of the $\text{Sr}_2\text{NaNb}_5\text{O}_{15}$ solid solution was derived using the Rietveld method. The refinements were performed taking into account the space groups P4bm (No 100), compatible with the rule of existence $[(0\ k\ l)\ k = 2n]$. Powder data and experimental conditions are listed in Table 3. R_{Bragg} , R_{F} , R_{p} and R_{wp} index values obtained from refinement of the $\text{Sr}_2\text{NaNb}_5\text{O}_{15}$ system are considered very good. The R_{p} index, $cR_{\text{wp}} = \left\{ \sum w_i (Y_o^i - Y_c^i)^2 / \sum w_i Y_o^i \right\}^{1/2}$ where w_i is the weight assigned at each intensity step, indicates the agreement between the structure model adopted and the real one. The R_{wp} index, $R_{\text{wp}} = \sum |Y_o^i - Y_c^i| / \sum Y_o^i$ where Y_o^i and Y_c^i are the observed and calculated intensities, respectively, indicates the quality of the refinement.

Table 3: Structural data of Sr₂NaNb₅O₁₅ and experimental conditions.

Crystallographic Data	
calcination temperature	1150°C
Time	12 h
Crystal system	Tetragonal
Space group	P4bm (100)
a [Å]	12.34568
c [Å]	3.89383
V [Å ³]	593.482
Data Collection	
Program	FullProf
Function for background level	Polynomial - 5 order
Function for peak shape ($H^2 = U \tan^2\Theta + V \tan\Theta + W$)	Pseudo-Voigt
R _{Bragg} (%)	3.59
R _F (%)	3.15
^c R _p (%)	9.82
^c R _{wp} (%)	13.1
χ^2	2.66

Figure 3 shows the Rietveld graph for Sr₂NaNb₅O₁₅ with the observed and derived X-ray diffraction, as well as their differences. The lattice parameters derived for Sr₂NaNb₅O₁₅ are equal to: $a = b = 12.3456 (6) \text{ \AA}$, $c = 3.8938 (2) \text{ \AA}$ and the volume $V = 593.482 (5) \text{ \AA}^3$ of tetragonal symmetry and space group P4bm (100).

The best theoretical adjustment for the Sr₂NaNb₅O₁₅ phase was obtained assuming that each pentagonal site (4c (x, x+1/2, z)) was statistically occupied by equal quantities of Na⁺ and Sr²⁺ ions and that each tetragonal site (2a (0,0,z)) was occupied by an Sr²⁺ ion. The trigonal site was considered vacant.

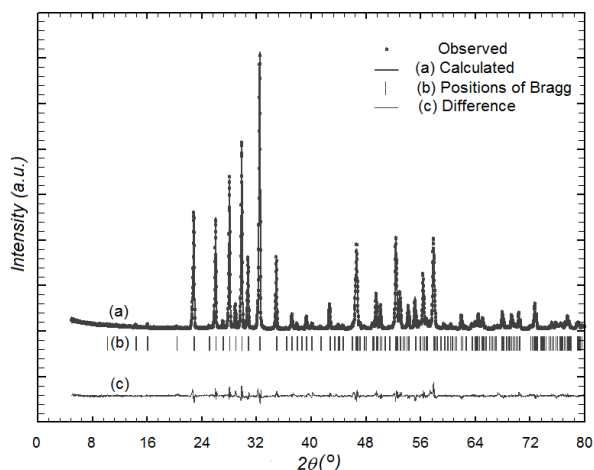


Figure 3. Rietveld graph for $\text{Sr}_2\text{NaNb}_5\text{O}_{15}$.

The atomic parameters obtained by refinement of the $\text{Sr}_2\text{NaNb}_5\text{O}_{15}$ are listed in Table 4.

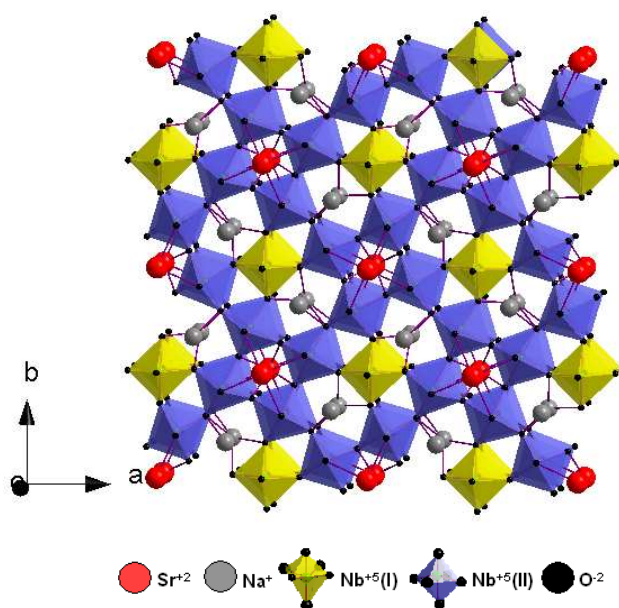
Refinement data obtained for the $\text{Sr}_2\text{NaNb}_5\text{O}_{15}$ precursor powder heated at 1150 °C several times for less than 12 h showed major isotropic thermal parameter B values (data not shown). Such phenomenon is compatible with a crystallization process in ceramic powders. Since the B parameter is related to the degree of order-disorder, a higher B value suggests a higher degree of disorder in the structure ⁽¹⁴⁾.

Therefore, it is possible to hypothesize that the $\text{Sr}_2\text{NaNb}_5\text{O}_{15}$ oxide prepared here exhibits a residual static disorder correlated to the crystallization process. This feature is compatible with a process of rearrangement and growth of crystallites from a sintering phenomenon of the nanostructures ⁽⁷⁾, as shown in Fig. 2. In this sense, some kind of order retrieving has been reported after thermal annealing of the disordered material, in which a degree of disorder was created by mechanical refinement of the crystallite size ⁽¹⁵⁾.

Table 4. Atomic coordinates and isotropic thermal parameters B (Å).

<i>Atoms</i>	<i>Wyckoff Position</i>	<i>x/a</i>	<i>y/b</i>	<i>z/c</i>	<i>B</i>
Sr(1)	2a	0	0	-0.01457 (4)	0.016 (3)
Na(2)	4c	0.17263 (2)	0.67263 (2)	-0.02115 (4)	0.055 (2)
Sr(2)	4c	0.17263 (2)	0.67263 (2)	-0.02115 (4)	0.055 (2)
Nb(1)	2b	0	½	½	0.034 (2)
Nb(2)	8d	0.07627 (3)	0.21104 (3)	0.47820 (2)	0.0131 (12)
O(1)	8d	0.13270 (9)	0.06722 (9)	0.37197 (3)	0.055 (4)
O(2)	8d	0.34232 (1)	0.00469 (8)	0.38305 (4)	0.055 (4)
O(3)	8d	0.08883 (1)	0.19947 (9)	-0.07274 (6)	0.055 (4)
O(4)	4c	0.28409 (8)	0.78409 (8)	0.43520 (9)	0.055 (4)
O(5)	2b	0	½	0.02700 (4)	0.055 (4)

Figure 4 shows the graphic representation of the unit cell obtained for the $\text{Sr}_2\text{NaNb}_5\text{O}_{15}$ solid powder solution, along a x b plane, from the data listed in Table 4. Niobium atoms are coordinated to six oxygen atoms, four of which are located, *a priori*, on the same plane as the niobium atoms, and the other two are above and below the plane, respectively. It is a favorable condition for the formation of an M site (octahedron) in the structure ⁽¹⁴⁾.

**Figure 4 .** Graph of the unit cell obtained for the $\text{Sr}_2\text{NaNb}_5\text{O}_{15}$ powder.

CONCLUSION

Modified polyol method is a suitable method of preparation of niobate nanocrystalline and single phase nanopowders with $\text{Sr}_2\text{NaNb}_5\text{O}_{15}$ TTB-type structure, which presents a space group compatible with P4bm (100) of tetragonal symmetry. The unitary cell showed that each pentagonal site is statistically occupied by equal quantities of Na^+ and Sr^{2+} ions and that each tetragonal site is occupied by an Sr^{2+} ion.

ACKNOWLEDGMENTS

FAPESP, CNPq, and Fundunesp for the financial support.

REFERENCES

- (1) PAZ DE ARAUJO, C. A.; CUCHIARO, J. D.; MCMILLAN, L. D.; SCOTT, M. C.; SCOTT, J. F.; Fatigue-free ferroelectric capacitors with platinum - electrodes, *Nature*, v. 374, p. 627 (1995).
- (2) CHEN, X. M.; SUZUKI, Y.; SATO, N. Sinterability Improvement of $\text{Ba}(\text{Mg}_{1/3}\text{Ta}_{2/3})\text{O}_3$ Dielectric Ceramics, *J. Mater. Sci.: Mater. Electron.*, v. 5, p. 244–47, 1994.
- (3) SLATER, P. R.; IRVINE, J. T. S. Synthesis and electrical characterisation of the tetragonal tungsten bronze type phases, $(\text{Ba}/\text{Sr}/\text{Ca}/\text{La})_{0.6} \text{M}_x \text{Nb}_{1-x} \text{O}_{3-\delta}$ (M = Mg, Ni, Mn, Cr, Fe, In, Sn): evaluation as potential anode materials for solid oxide fuel cells. *Solid State Ionics*, v. 124, p. 61, 1999.
- (4) TRIBOTTÉ, B.; HAUSSONNE, J. M.; DESGARDIN, G. $\text{K}_2\text{Sr}_4\text{Nb}_{10}\text{O}_{30}$ -based dielectric ceramics having the tetragonal tungsten bronze structure and temperature-stable high permittivity, *J. Eur. Ceram. Soc.*, v.19, p. 1105-1109, 1999.
- (5) ABRAHAMS, S. C.; JAMIESON, P. B.; BERNSTEIN, J. L. Ferroelectric tungsten bronze-type crystal structures III. Potassium lithium niobate $\text{K}_{(6-x-y)}\text{Li}_{(4+x)}\text{Nb}_{(10+y)}\text{O}_{30}$. *J. Chem. Phys.*, v. 54, p. 2355-64, 1971.
- (6) WAKIYA, N.; WANG, J. K.; SAIKI, A.; SHINOZAKI, K.; MIZUTANI, N. Synthesis and Dielectric Properties of $\text{Ba}_{1-x}\text{R}_{2x/3}\text{Nb}_2\text{O}_6$ (R: Rare Earth) with Tetragonal Tungsten Bronze Structure. *J. Eur. Ceram. Soc.*, v. 19, p. 1071, 1999.
- (7) LANFREDI, S.; CARDOSO, C. X.; NOBRE, M. A. L.; Crystallographic properties of $\text{KSr}_2\text{Nb}_5\text{O}_{15}$, *Mat. Sci. Eng. B*, v. 112, p. 139-143, 2004.

(8) CARVAJAL, J. R., An introduction to the program FullProff 2000 (version May 2008), **Laboratoire Léon Brillouin (CEA-CNRS) CEA/Saclay**, 91191 Gif sur Yvette Cedex, FRANCE.

(9) CAGLIOTI, G.; PAOLETTI, A.; RICCI, F. P., Choice of collimators for a crystal spectrometer for neutron diffraction, **Nuclear Instruments**, v. 3(4), p. 223-228, 1958.

(10) DIAMOND, Crystal and Molecular Structure Visualization, Crystal Impact, Inc. 1998-2009.

(11) Jade 8 Plus, XRD Pattern Processing, Identification & Quantification, **Materials Data, Inc.**, Copyright^(c), 1995-2007.

(12) FARREL, F. I.; MARONI, V. A.; SPIRO, T. G.; Vibrational analysis for Nb₆O₁₉₋₈ and Ta₆O₁₉₋₈ and the Raman intensity criterion for metal-metal interaction. **Inorg. Chem.** 1969, 8, 2638.,

(13) CORDIER, S.; HERNANDEZ, O.; THÉPOT, J.Y.; SHAMES, A.I.; PERRIN, C. Synthesis, crystal structure, and characterization of the first Nb(3) triangular cluster compound bonded to fluorine ligands: association of Nb(3)I(i)F(i)(3)F(a)(8)L(a) units and Nb(IV)L(6) Octahedra with L=O and F. **Inorg. Chem.** v. 42, p. 1101-1106, 2003.

(14) BELGHITI, ALAOUI EL H. et al., Ferroelectric and crystallographic properties of the Sr_{2-x}K_{1+x}Nb₅O_{15-x}F_x solid solution, **Solid State Sciences**, v. 4, p. 933-940, (2002).

(15) X. Gao, J. Xue, T. Yu, Z. Shen, J. Whang, B-Site Order–Disorder Transition in Pb(Mg_{1/3}Nb_{2/3})O₃–Pb(Mg_{1/2}W_{1/2})O₃ Triggered by Mechanical Activation, **J. Am. Ceram. Soc.**, v. 85, p. 833-838, 2002.